IEEE Access
Multidisciplinary | Rapid Review | Open Access Journal

Received 23 September 2024, accepted 21 November 2024, date of publication 27 November 2024,
date of current version 10 December 2024.

Digital Object Identifier 10.1109/ACCESS.2024.3507535

RESEARCH ARTICLE

Polarimetric Vegetation Propagation Measurements on a Brazilian University Campus Scenario

GLAUCIO L. RAMOS[1], NUNO R. LEONOR[2,3], LUIZ DA SILVA MELLO[4], (Member, IEEE), FERNANDO J. S. MOREIRA[5], (Senior Member, IEEE), CASSIO G. REGO[5], SANDRO T. M. GONCALVES[6], AND RAFAEL F. S. CALDEIRINHA[2,3], (Senior Member, IEEE)

[1]DETEM–PPGEL, Federal University of São João Del-Rei, Ouro Branco 36495-000, Brazil
[2]Instituto de Telecomunicações, 3810-193 Leiria, Portugal
[3]Polytechnic of Leiria, 2411-901 Leiria, Portugal
[4]DEE, Pontifical Catholic University of Rio de Janeiro (PUC-Rio), Rio de Janeiro 22451-900, Brazil
[5]DELT, Federal University of Minas Gerais, Belo Horizonte 31270-901, Brazil
[6]DEE–PPGEL, Federal Center for Technological Education of Minas Gerais, Belo Horizonte 30575-180, Brazil

Corresponding author: Glaucio L. Ramos (glopesr@gmail.com)

The Article Processing Charge for publishing this research was funded by the Coordination for the Improvement of Higher Education Personnel - CAPES (ROR identifier: 00x0ma614).

ABSTRACT This paper discusses a polarimetric measurement campaign conducted in two distinct environments, with data collected at the Federal University of Minas Gerais (UFMG) in Brazil. The study investigates millimeter wave propagation through vegetation at a frequency of 36.6 GHz in two scenarios: the Central Square of UFMG and a forested area within the campus. In the first scenario, measurements were conducted along a main street with varying degrees of vegetation obstruction, focusing on analysing fast fading. For the fast-fading analysis, Rayleigh, Rice, and m-Nakagami distributions were considered. Results from the first scenario indicate that the m-Nakagami distribution provides the best fit for both vertical and horizontal polarisations, surpassing traditional models such as Rayleigh and Rice. In the second scenario, measurements were taken within a forested area, and the study was undertaken to analyse fast fading and excess loss. Considering the excess loss study, measurements were compared with three traditional models (CCIR, Weissberger, and COST 235). Excess loss analysis showed that traditional excess loss propagation models tend to exhibit a minimum RMS error of 10.6 dB for vertical polarisation and 15 dB for horizontal polarisation (Weissberger model), whereas the proposed model demonstrated improved accuracy over log-distance models, particularly for vertical polarisation, presenting an RMS error of 5.8 dB, and for the horizontal polarisation a RMS error of 10.2 dB, at least 4.8 dB smaller than the Weissberger model. Considering the fast fading analysis, the m-Nakagami distribution tends to provide better results in both polarisation. These findings underscore the importance of accurate propagation models tailored to specific environmental conditions, such as vegetation, to enhance the reliability of future 5G evolution and 6G microwave communication systems.

INDEX TERMS Polarimetric measurements, vegetation scenario, fast fading analysis.

I. INTRODUCTION

At present, mobile communication systems operate within the millimeter-wave frequency range and preliminary

The associate editor coordinating the review of this manuscript and approving it for publication was Weiren Zhu.

investigations are underway for the development of the sixth generation (6G). A prevailing trend in modern systems is their operation at higher frequency bands, prompting propagation studies across centimeter, millimeter, and sub-THz frequency ranges.

Focusing on the microwave and millimeter-wave frequency band, wireless technology can be classified into two main frequency ranges: FR1 (410 to 7125 MHz) and FR2 (24.25 to 52.6 GHz) [1]. FR1 primarily consists of the sub-6 GHz spectrum, which provides a balance between range and performance for 5G applications. FR2 offers higher performance for 5G and future 6G applications due to the availability of larger bandwidths, which can deliver higher data rates and lower latency. Within FR2, the 36.6 GHz range is notable for its applications in various fields, including 5G networks, automotive radar systems, satellite communications, point-to-point communications, remote sensing, and certain industrial applications [2], [3], [4], [5].

The impact of vegetation on signal propagation has been a subject of scrutiny across various wireless communication generations, spanning from the inception of these systems to their current evolution. This emphasis on vegetation-related effects remains crucial for developing future communication systems.

Modeling propagation through vegetation is challenging due to the numerous propagation mechanisms in real environments, such as penetration, ground reflection, multi-scattering, diffraction around vegetation, and forward scattering along the boundaries of vegetated areas [2], [3], [4], [6].

The existing literature contains numerous studies on signal propagation through vegetative environments. For example, a generic model of 1-60 GHz radio propagation through vegetation was proposed in [7]. Also, a measurement campaign at the 5G millimeter-wave frequency band was conducted in two vegetated suburban macro-cell areas, leading to the development of an angle-based path loss characterisation that improved 3GPP models for these scenarios [8]. Another study proposed a simplified propagation model considering direct transmission through a succession of trees and transmission across the forest canopy, which outperformed the RET model for both short and long path lengths [6].

Additionally, a measurement campaign using a 60 GHz channel sounder was conducted to calibrate a ray-tracing propagation model for summer and winter tree conditions, accurately predicting foliage loss [9]. Further studies explored suburban tree clutter attenuation at 24 GHz [10], signal attenuation at 28 GHz in vegetated environments [11], and a millimeter-wave foliage propagation model [12]. In [13], it was proposed that a combined ITM and LITU-R model be used to perform radio coverage prediction in mountain-vegetated areas. Collectively, these studies enhance our understanding of the complex interactions between wireless signals and vegetation, which is essential for advancing communication technologies.

While polarisation aspects have been studied for wireless communication systems, for example [14], [15], [16], and [17], polarimetric propagation studies in vegetation-rich areas are relatively sparse. Notable contributions include a study presenting measurement results for a 39 GHz millimeter-wave dual-polarised channel under foliage conditions [4]. Given the ongoing operation of 5G networks and the anticipated use of the millimeter-wave frequency band for 6G, continuous experimental campaigns examining wave polarisation in vegetated scenarios are crucial.

This research endeavors to contribute to the field by presenting results from a polarimetric study conducted at 36.6 GHz, focusing on vegetation environments within a university campus in Belo Horizonte, MG, Brazil. The primary contributions of this study can be briefly summarized as:

- A polarimetric study assessing propagation loss within a small forest wedge at a millimeter-wave frequency band, proposing different models for each polarisation case.
- A polarimetric examination of large-scale propagation probability in two distinct vegetation environments, operating within a millimeter-wave frequency band.

The paper is structured as follows: Section II outlines the measurement setup, Section III provides a detailed description of the measurement scenarios, and Section IV presents the measurement results along with the analysis for both propagation loss and large-scale probability best fit. Finally, Section V encapsulates the conclusions drawn from both studies.

II. MEASUREMENT SETUP

In this research, the development of the vegetation propagation model for millimeter wave coverage predictions was based on experimental data collected during a measurement campaign at the Federal University of Minas Gerais (UFMG) in Belo Horizonte, Brazil. This campaign involved polarimetric measurements of the received signal level in two distinct scenarios with vegetation, conducted at a frequency of 36.6 GHz.

The transmitter (TX) setup included two distinct signals separated by 10 kHz, facilitating a polarimetric measurement campaign with simultaneous transmission of both vertical and horizontal polarisations, as illustrated in Fig. 1. The 10 kHz spacing allows the simultaneous transmission of both components without cross-polarization interference, and at the receiver, the SA span window enables the visualization and acquisition of both components (quasi) simultaneously.

The vertically transmitted signal was generated using an Anritsu 68167C signal generator, producing continuous-wave (CW) signals at 5 dBm, tuned to the specified 36.6 GHz frequency. Additionally, another signal was generated from the TX block, comprising a PLL centered around 18 GHz, a frequency doubler, a mixer, and power amplifiers, thereby creating another CW frequency at 36.600010 GHz. Both signals were transmitted with different polarisations (H and V) using an RFSpin QRH0140 directional antenna.

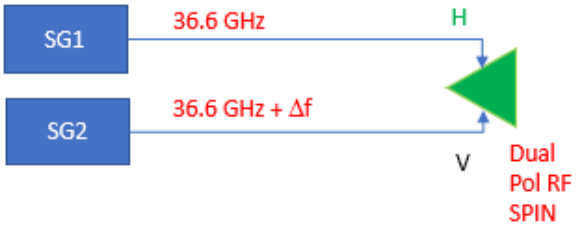

FIGURE 1. Transmitter block diagram.

Both transmitted signals were received using an RFSpin QRH0140 antenna on the reception side. An Anritsu MS2668C spectrum analyser was employed to capture the VV and HV received signals at 36.6 and 36.600010 GHz, representing the vertically transmitted signal received in both vertical and horizontal polarisations. For receiving the horizontally transmitted signal in both horizontal and vertical polarisations, an Agilent N9000A CXA spectrum analyser was utilised. In this case, the received signals were down-converted and identifiable at 200 MHz and 200.010 MHz, as shown in Fig. 2.

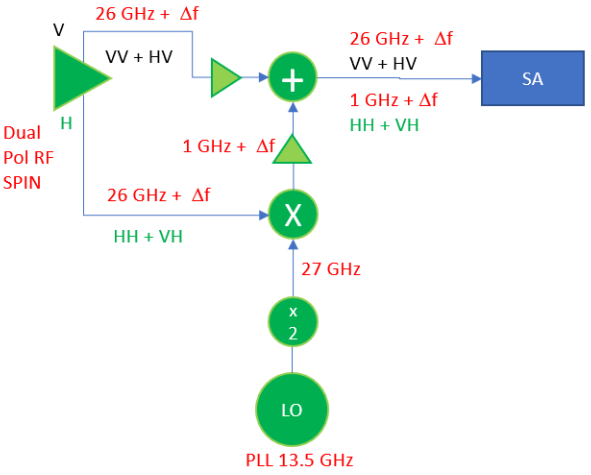

FIGURE 2. Receiver block diagram.

III. MEASUREMENT SCENARIOS

The experimental data were acquired in two distinct scenarios. In the first scenario, the transmitter (TX) was positioned at the UFMG Central Square, as illustrated in Fig. 3. Some images were obtained from Open Street Map and other were taken in the field. The TX antenna was placed at a height of 2.13 m, transmitting a 5 dBm continuous-wave (CW) signal. The measurement was conducted along the main street in both directions (orange lines). This street also serves as a parking area, with several trees and cars. Consequently, throughout most of the measured route, vegetation likely obstructed the received signal. The probability density function (PDF) and cumulative density function (CDF) for fast fading variation were estimated for both the left and right sides of the main street.

(a)

(b)

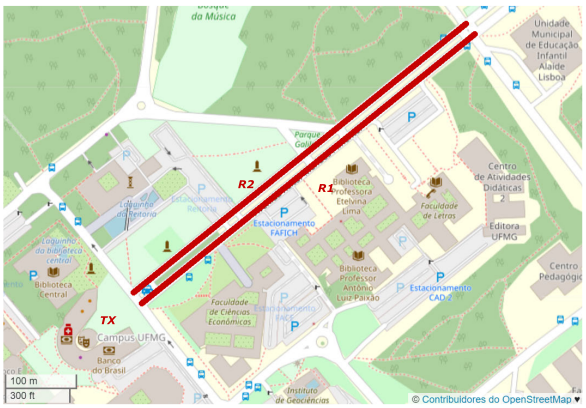

(c)

FIGURE 3. UFMG Central Square Measurement first scenario (a) Central square view, (b) RX view, (c) Schematic for measurements.

The second scenario took place in a small wedge forest within the university campus, depicted in Fig. 4, with

some views obtained from Open Street Map and some pictures taken in the field. The TX antenna was strategically positioned at eight different sectors at one corner of the small forest, at a height of 2.13 m. Four measurements were conducted at various positions for each sector, with an RX antenna height of 2.90 m. With this set of sectors, the antenna's main lobe effectively illuminated all measurement locations through its main lobe. All measurements, separated by 1 m, were carried out on the opposite side of the wedge, ensuring that all positions were obstructed by vegetation and this way obtaining varying vegetation depths to evaluate the path decay with both antennas at boresight.

In this scenario, excess vegetation loss was estimated and compared with traditional vegetation models. Additionally, the probability density function (PDF) and cumulative density function (CDF) for fast fading variation were estimated for this scenario, considering a measurement run on one side of the wedge, with the TX antenna positioned at the corner of the wedge.

IV. MEASUREMENT RESULTS AND ANALYSIS

In the first scenario, a fast fading analysis was conducted, and the probability density function (PDF) and cumulative density function (CDF) were obtained for two distinct routes on the main street (R1 on the right side of the street away the TX and R2 on the left toward TX). To perform this fast-fading statistical analysis, the received power signal (in dBm) was first converted to linear units (Watts), and then a proportional voltage signal was derived. A low-pass filtering (mean average) was applied to the signal to remove slow variations, and the signal was normalised with respect to its estimated modal value. These PDFs were then compared with traditional Rayleigh, Rice, and m-Nakagami distributions, as described by Eqs. (1)-(3).

$$p(r) = \frac{r}{\sigma^2} exp\left(-\frac{r^2}{2\sigma^2}\right) \tag{1}$$

$$p(r) = \frac{r}{\sigma^2} exp\left(-\frac{r^2+s^2}{2\sigma^2}\right) I_0\left(\frac{rs}{\sigma^2}\right) \tag{2}$$

$$p(r) = \frac{2m^m r^{2m-1}}{\Gamma(m)\Omega^m} exp\left(-\frac{mr^2}{\Omega}\right) \tag{3}$$

The same analysis was carried out for both vertical and horizontal polarisations to determine the best fit for each polarisation. For the first scenario, 1781 measurement samples were obtained for Route R1 and 1988 samples for Route R2. The parameters for each distribution were estimated using JupyterLab (Python language), and the results for routes R1 and R2, respectively, considering both polarisations, are presented in Tables 1 and 2.

The estimated PDFs and CDFs for each considered probability distribution are compared with the measured signal, as shown in Figure 5 and Figure 6.

To characterise the statistical distribution that best fits the measurement fast fading data, the Kullback-Leibler divergence (KLD) test [18] was applied to compare the empirical cumulative distribution to the theoretical Rayleigh, Rice, and m-Nakagami distributions.

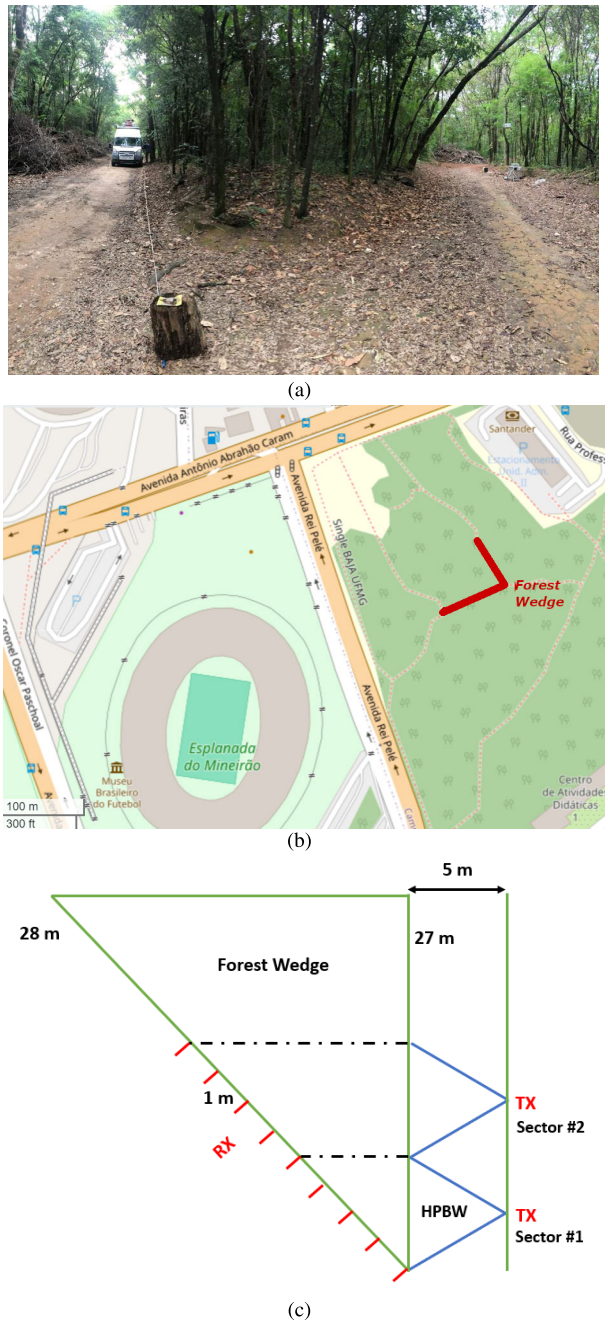

FIGURE 4. UFMG Forest - second scenario (a) forest wedge view, (b) forest top view, (c) Schematic for measurements.

TABLE 1. Probability function parameters for route 1, VV and HH polarisation.

Distribution	VV polarisation	HH polarisation
Rayleigh	σ = 0.7703	σ = 0.7837
Rice	s = 0.7770 / σ = 0.5399	s = 0.0342 / σ = 0.7833
Nakagami	m = 1.3671 / Ω = 1.1867	m = 0.9355 / Ω = 1.2283

TABLE 2. Probability function parameters for Route 2, VV and HH polarisation.

Distribution	VV polarisation	HH polarisation
Rayleigh	$\sigma = 0.8088$	$\sigma = 0.8271$
Rice	s = 0.7868 / $\sigma = 0.5870$	s = 0.6175 / $\sigma = 0.7024$
Nakagami	m = 1.3080 / $\Omega = 1.3082$	m = 1.1598 / $\Omega = 1.3682$

The KLD test is a measure of how one probability distribution diverges from another [18]. The formulation is described by Eq. 4:

$$D_{KL}(P \parallel Q) = \sum_i P(i) \log \frac{P(i)}{Q(i)}, \tag{4}$$

where if $D_{KL} = 0$, the distributions P and Q distributions are identical. If $D_{KL} > 0$, there is a difference between the distributions, with greater values indicating a larger difference between them.

Results for the KLD for routes R1 and R2, respectively, considering both polarisations, are presented in Table 3.

TABLE 3. Kullback-Leibner Test - Scenario 1.

Distribution	R1-VV	R1-HH	R2-VV	R2-HH
Rayleigh	0.0030	0.000366	0.0026	0.0012
Rice	0.0009	0.000366	0.0034	0.0009
Nakagami	8.7×10^{-5}	0.000358	0.0001	0.0003

From the measurement results and KLD tests, it can be concluded that for both R1 and R2 routes on the main street of the Central Square at UFMG (Scenario 1), the m-Nakagami distribution provides the best fit for both vertical (V) and horizontal (H) polarisations, as the KL divergence result was closer to zero for the m-Nakagami distribution for all considered cases.

To enhance the technical interpretation of the obtained fast fading results, a heat map was simulated for all the collected data. In Figure 7, the estimated m-Nakagami probability distribution is shown in the background, and the measured fast fading is also presented overlaid on this distribution. The probability value is represented by the color scale. It is evident that the majority of the fading signal is concentrated around the 80-90% probability region.

Moving on to the second scenario, illustrated in Fig. 4 which involves the forest wedge, an initial analysis was conducted for excess loss due to vegetation. In this context, the best-fit analysis will be compared with three different reference models: (a) the International Telecommunication Union Radiocommunication Sector (CCIR) model for propagation in vegetation [19], (b) the COST 235 model [20], and (c) Weissberger model [21]. All three models are based on the formulation described by Equation 5,

$$L_v = a \cdot f^b \cdot d_v^c, \tag{5}$$

where f is the frequency, in GHz, and d is the vegetation depth, in meters, with the parameters outlined in Table 4.

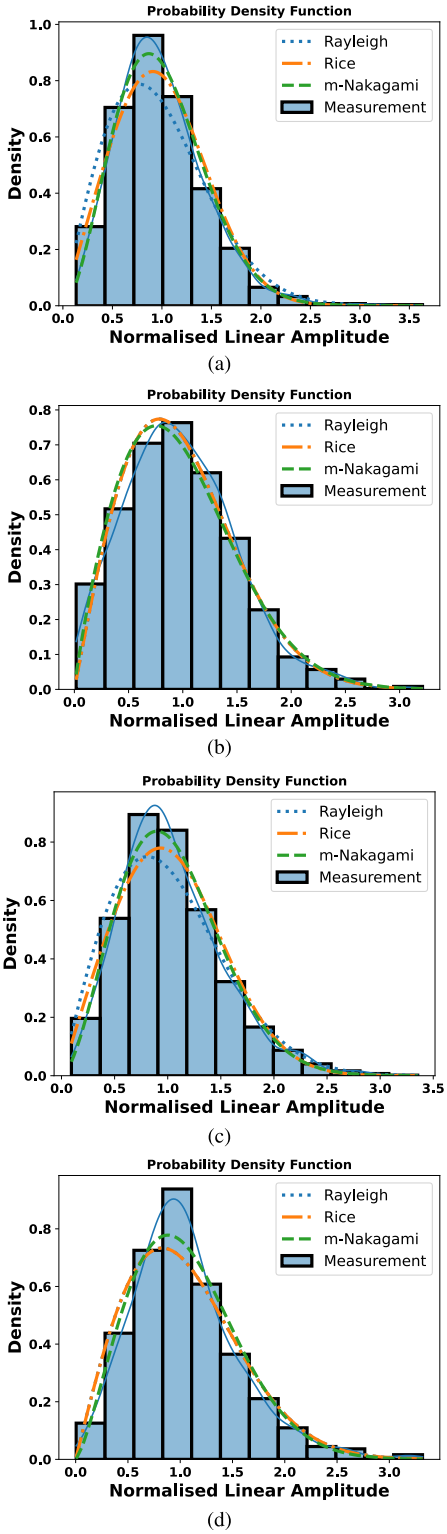

FIGURE 5. UFMG Central Square pdf analysis for (a) route R1 - VV, (b) route R1 - HH, (c) route R2 - VV, and (d) route R2 - HH.

Additionally, a new model is proposed, based on the adjusted coefficients of Equation 5.

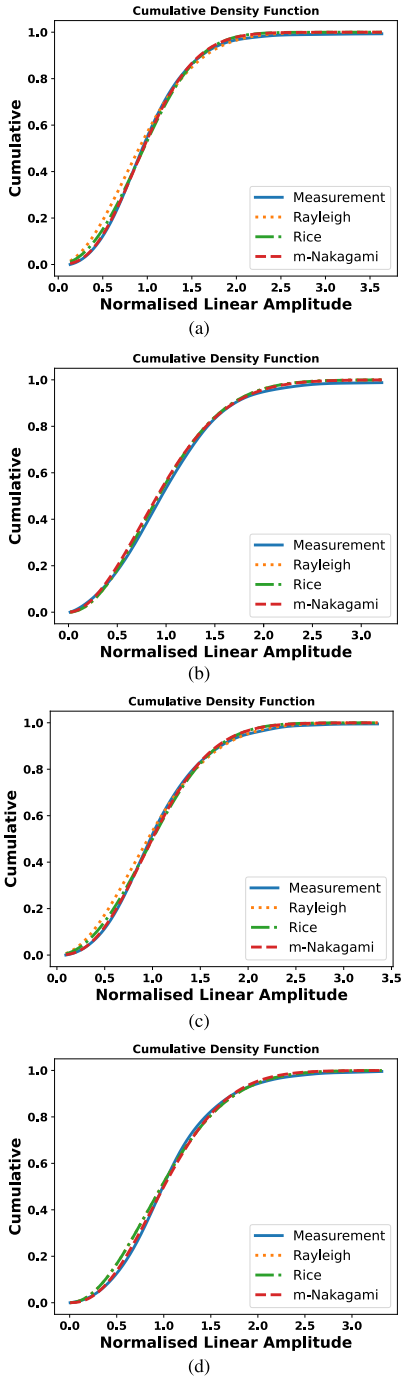

FIGURE 6. UFMG Central Square cdf analysis for (a) route R1 - VV, (b) route R1 - HH, (c) route R2 - VV, and (d) route R2 - HH.

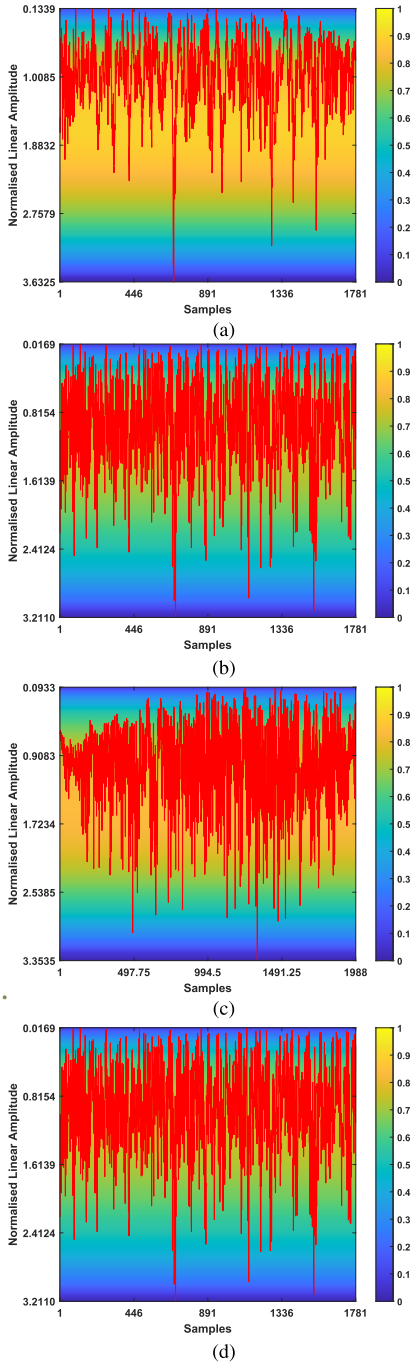

FIGURE 7. UFMG Central Square m-Nakagami probability density and measured fast fading, for (a) route R1 - VV, (b) route R1 - HH, (c) route R2 - VV, and (d) route R2 - HH.

TABLE 4. Summary of the considered vegetation models.

Models	Parameters		
	a	b	c
CCIR	0.2	0.3	0.6
COST 235	13.77	-0.009	0.26
Weissberger	1.33	0.284	0.588

A traditional log-distance model was also considered for each polarisation, and the obtained equations for the log-distance and the proposed model for vertical and horizontal polarisation cases can be seen in Equations 6 and 7, respectively.

$$\begin{aligned} Proposed: L_v[dB] &= 1.127 \cdot f^{0.5512} \cdot d^{0.1753}, \\ Log-Distance: L[dB] &= \\ &-22.7868 - 33.28log(d/8.8304). \end{aligned} \tag{6}$$

$$Proposed : L_v[dB] = 3.062 \cdot f^{-0.5786} \cdot d^{1.246},$$
$$Log - Distance : L[dB] = - 52.3010 - 24.45log(d/8.8304). \quad (7)$$

The path loss exponent (PLE) for the vertical polarisation and horizontal polarisation were, respectively, 3.328 and 2.445.

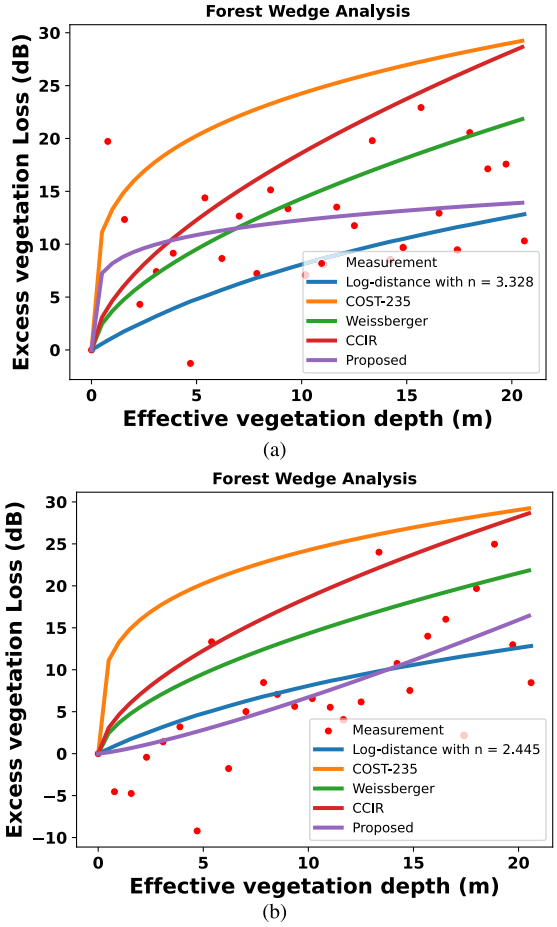

FIGURE 8. Excess vegetation loss at UFMG Forest scenario for (a) VV and (b) HH polarisations.

The measured excess loss compared to traditional models is depicted in Figure 8 for vertical and horizontal polarisation, respectively. Additionally, a mean average error (MAE) and a root mean square error (RMSE) analyses were conducted for vertical and horizontal polarisations, with the results presented in Tables 5 and 6, respectively. Traditional models exhibited a high RMS error when compared to the measurements, ranging from at least 10.6 dB for vertical polarisation to 15.0 dB for horizontal polarisation in the case of the Weissberger model. In contrast, the log-distance best-fit proposed model shows an improvement of at least 4.7 dB for vertical polarisation and 8.8 dB for horizontal polarisation. It is also noteworthy that the proposed model,

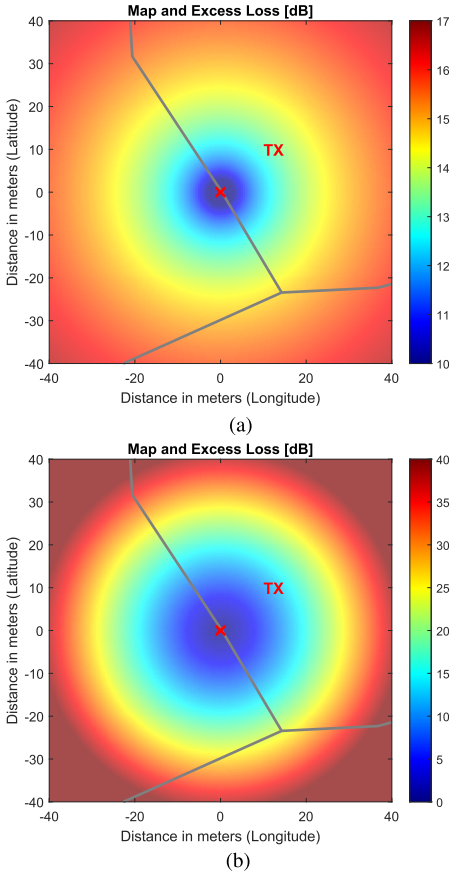

FIGURE 9. UFMG Forest wedge excess path loss map for (a) Proposed VV and (b) Proposed HH.

based on the adjustment of the coefficients of Equation 5, yields a smaller error than the log-distance based model, but only for vertical polarisation.

TABLE 5. MA and RMS error for the vertical polarisation [dB].

Model	MAE [dB]	RMSE [dB]
Proposed	4.7	5.8
Log Distance	5.1	6.7
COST 235	16.8	17.6
Weissberger	9.5	10.6
CCIR	15.6	16.6

TABLE 6. MA and RMS Error for the horizontal polarisation [dB].

Model	MAE [dB]	RMSE [dB]
Proposed	9.1	10.2
Log Distance	4.6	6.2
COST 235	21.5	22.5
Weissberger	13.8	15.0
CCIR	20.2	21.0

An additional simulation was conducted to illustrate the excess path loss map around a transmitter in the forest wedge

scenario. Excess path loss maps were generated for the proposed VV and HH polarizations, with the transmitter's coordinates serving as the origin of the coordinate system (distance). The differences in excess loss across all analyzed models are shown in Figure 9.

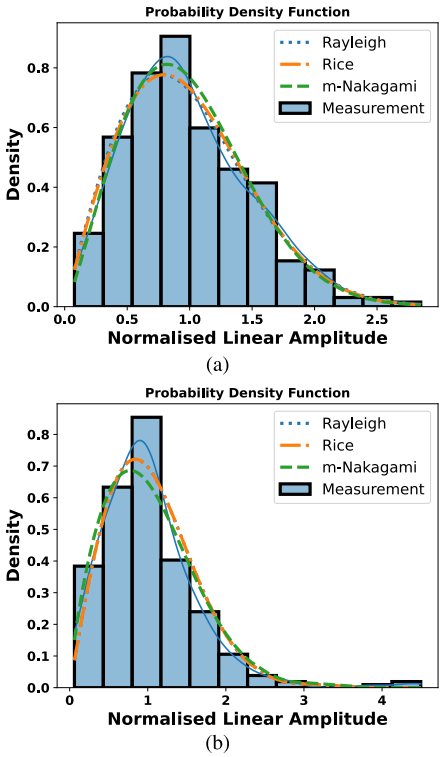

FIGURE 10. UFMG Forest wedge pdf analysis for (a) VV and (b) HH polarisations.

In addition to the excess loss analysis, a fast-fading analysis was performed for the forest wedge scenario. The TX antenna was positioned for each 8 sectors, and the RX antenna was positioned in the main lobe of the TX antenna, within a distance of 1 m for each measurement. When the next RX position was not in the main lobe, the TX antenna was moved to another sector, as can be illustrated in Fig. 4. A total of 282 fast variation measurements were processed. The PDFs and CDFs were obtained for both polarisations and compared with traditional Rayleigh, Rice, and m-Nakagami distributions. The estimated parameters for each distribution for vertical and horizontal polarisation are presented in Table 7. The comparison of PDFs and CDFs with measurements is depicted in Figures 10 and 11.

Results for the KLD test for the forest wedge scenario, considering both polarisations, are presented in Table 8. The KLD results once again indicate that the m-Nakagami distribution provides a better fit for all polarisations in the presence of a vegetation-obstructed path, as the KL divergence results were closer to zero for the m-Nakagami distribution for all considered cases.

TABLE 7. Probability function parameters for forest wedge, VV and HH polarisation.

Distribution	VV polarisation	HH polarisation
Rayleigh	$\sigma = 0.7799$	$\sigma = 0.8407$
Rice	s = 0.5090/ $\sigma = 0.6919$	s = 0.0087 / $\sigma = 0.8406$
Nakagami	m = 1.1145 / $\Omega = 1.2165$	m = 0.8714 / $\Omega = 1.1462$

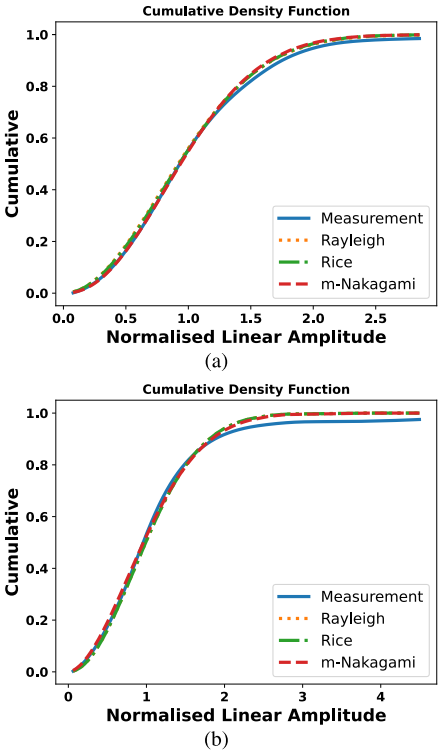

FIGURE 11. UFMG Forest wedge cdf analysis for (a) VV and (b) HH polarisations.

TABLE 8. Kullbak-Leibner Test - Scenario 2.

Distribution	Forest - VV	Forest - HH
Rayleigh	0.0003	0.0005
Rice	0.0002	0.0005
Nakagami	8.3×10^{-5}	0.0002

Once again, to enhance the technical interpretation of the obtained fast fading results for the forest scenario, a heat map was simulated for all the collected data. In Figure 12, the estimated m-Nakagami probability distribution is shown in the background, and the measured fast fading is also presented overlaid on this distribution. The probability value is represented by the color scale. It is evident that the majority of the fading signal is concentrated around the 80-90% probability region.

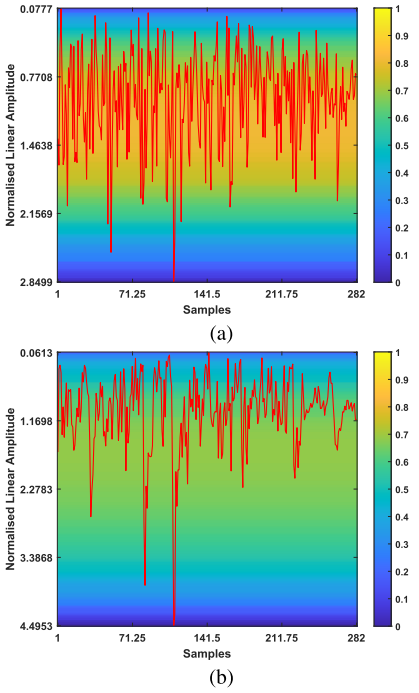

FIGURE 12. UFMG Forest wedge m-Nakagami probability density and measured fast fading for (a) VV and (b) HH polarisations.

V. CONCLUSION

A polarimetric measurement campaign was conducted at 36.6 GHz in two vegetation environments within a university campus scenario. In the main street of the central square, a thorough analysis of fast fading was executed for both vertical and horizontal polarisations. The results revealed that the m-Nakagami distribution offered the best fit for the multipath obstructed environment with vegetation, as they presented a smaller KL divergence result, demonstrating its suitability for both polarisations.

Two distinct analyses were undertaken for the small forest wedge scenario within the university campus. Firstly, the best fit of the excess loss measurement was compared with three traditional propagation models. The observed high RMSE when applying these models emphasized the necessity for developing a more accurate propagation model for similar environments at this frequency range, for both polarisations. Secondly, a fast-fading analysis showed that the Rayleigh distribution provided the best fit for vertical polarisation measurements, while the m-Nakagami distribution was once again the optimal fit for the horizontal case.

It is also important to emphasize the significance of the proposed model, which shows a considerable reduction in RMS error compared to traditional vegetation propagation models. For both polarisations, the proposed model presented an RMSE reduction of 4.8 dB when compared to the Weissberger model. As an important contribution, results showed that for the vertical polarisation the proposed model best fits the log-distance approximation, as it uses a different equation to adjust the model. Considering horizontal polarisation, log-distance fitted better, but once more the proposed model presented a smaller error when considering tradition vegetation models. Another key contribution of this study is the proposal of different models for each polarisation. Notably, for the horizontal polarisation case, the traditional models exhibited significantly higher RMS error, as these models do not account for polarisation changes. In the fast fading analysis, the results clearly indicate that the Rayleigh and Rice distributions are not the best fits for the environment under study in the millimeter-wave frequency band, whereas the m-Nakagami distribution tends to provide better results in both polarisations.

The polarisation dependency is associated with differences in scattering: vertical polarisation tends to align more with trunks and main branches, while horizontal polarisation interacts more with leaves and smaller branches. When radio waves pass through vegetation, their polarisation changes due to the multiple reflections occurring within the vegetation volume.

ACKNOWLEDGMENT

The authors would like to thank Paulo Pereira, Rogério do Nascimento Filho, and Jaci Nascimento for their support in the measurements campaign.

REFERENCES

[1] R. Dilli, "Analysis of 5G wireless systems in FR1 and FR2 frequency bands," in *Proc. 2nd Int. Conf. Innov. Mech. Ind. Appl. (ICIMIA)*, Mar. 2020, pp. 767–772.

[2] F. D. Diba, M. A. Samad, and D.-Y. Choi, "Centimeter and millimeter-wave propagation characteristics for indoor corridors: Results from measurements and models," *IEEE Access*, vol. 9, pp. 158726–158737, 2021.

[3] G. R. Maccartney, T. S. Rappaport, S. Sun, and S. Deng, "Indoor office wideband millimeter-wave propagation measurements and channel models at 28 and 73 GHz for ultra-dense 5G wireless networks," *IEEE Access*, vol. 3, pp. 2388–2424, 2015.

[4] Y. Lv, X. Yin, C. Zhang, and H. Wang, "Measurement-based characterization of 39 GHz millimeter-wave dual-polarized channel under foliage loss impact," *IEEE Access*, vol. 7, pp. 151558–151568, 2019.

[5] Y. Shen, Y. Shao, L. Xi, H. Zhang, and J. Zhang, "Millimeter-wave propagation measurement and modeling in indoor corridor and stairwell at 26 and 38 GHz," *IEEE Access*, vol. 9, pp. 87792–87805, 2021.

[6] R. Zabihi and R. G. Vaughan, "Simplifying through-forest propagation modelling," *IEEE Open J. Antennas Propag.*, vol. 1, pp. 104–112, 2020.

[7] N. Rogers, A. Seville, J. Richter, D. Ndzi, N. Savage, R. Caldeirinha, A. Shukla, M. Al-Nuaimi, K. Craig, E. Vilar, and J. Austin, "A generic model of 1–60 GHz radio propagation through vegetation-final report," Radiocommunications Agency, Groningen, Tech. QINETIQ/KI/COM/CR020196/1.0, 2002.

[8] P. Zhang, B. Yang, C. Yi, H. Wang, and X. You, "Measurement-based 5G millimeter-wave propagation characterization in vegetated suburban macrocell environments," *IEEE Trans. Antennas Propag.*, vol. 68, no. 7, pp. 5556–5567, Jul. 2020.

[9] C. Lai, D. Senic, C. Gentile, J. Senic, and N. Golmie, "Raytracing digital foliage at millimeter-wave: A case study on calibration against 60-GHz channel measurements on summer and winter trees," *IEEE Access*, vol. 11, pp. 145931–145943, 2023.

[10] I. Rodriguez, R. Abreu, E. P. L. Almeida, M. Lauridsen, A. Loureiro, and P. Mogensen, "24 GHz cmwave radio propagation through vegetation: Suburban tree clutter attenuation," in *Proc. 10th Eur. Conf. Antennas Propag. (EuCAP)*, Apr. 2016, pp. 1–5.

[11] J. Ko, Y.-S. Noh, Y.-C. Kim, S. Hur, S.-R. Yoon, D. Park, K. Whang, D.-J. Park, and D.-H. Cho, "28 GHz millimeter-wave measurements and models for signal attenuation in vegetated areas," in *Proc. 11th Eur. Conf. Antennas Propag. (EUCAP)*, Mar. 2017, pp. 1808–1812.

[12] F. Wang and K. Sarabandi, "An enhanced millimeter-wave foliage propagation model," *IEEE Trans. Antennas Propag.*, vol. 53, no. 7, pp. 2138–2145, Jul. 2005.

[13] N. Leonor, S. Faria, M. Vala, and R. F. S. Caldeirinha, "A combined ITM and LITU-R model for enhanced radio coverage predictions of mission-critical communications in mountainous vegetated terrains," *IEEE Antennas Wireless Propag. Lett.*, vol. 21, pp. 1777–1781, 2022.

[14] A. Maltsev, E. Perahia, R. Maslennikov, A. Sevastyanov, A. Lomayev, and A. Khoryaev, "Impact of polarization characteristics on 60-GHz indoor radio communication systems," *IEEE Antennas Wireless Propag. Lett.*, vol. 9, pp. 413–416, 2010.

[15] A. P. Garcia Ariza, R. Müller, F. Wollenschläger, A. Schulz, M. Elkhouly, Y. Sun, S. Glisic, U. Trautwein, R. Stephan, J. Müller, R. S. Thomä, and MatthiasA. Hein, "60 GHz ultrawideband polarimetric MIMO sensing for wireless multi-gigabit and radar," *IEEE Trans. Antennas Propag.*, vol. 61, no. 4, pp. 1631–1641, Apr. 2013.

[16] E. M. Vitucci, F. Mani, V. Degli-Esposti, and C. Oestges, "Polarimetric properties of diffuse scattering from building walls: Experimental parameterization of a ray-tracing model," *IEEE Trans. Antennas Propag.*, vol. 60, no. 6, pp. 2961–2969, Jun. 2012.

[17] X. Yin, Y. He, C. Ling, L. Tian, and X. Cheng, "Empirical stochastic modeling of multipath polarizations in indoor propagation scenarios," *IEEE Trans. Antennas Propag.*, vol. 63, no. 12, pp. 5799–5811, Dec. 2015.

[18] F. Perez-Cruz, "Kullback-leibler divergence estimation of continuous distributions," in *Proc. IEEE Int. Symp. Inf. Theory*, Jul. 2008, pp. 1666–1670.

[19] "Influences of terrain irregularities and vegetation on troposphere propagation," CCIR Report, Geneva, Switzerland, Rep. 235-236, 1986.

[20] European Commission, "Directorate-general for the information society and media, cost 235: Radiowave propagation effects on next-generation fixed-services terrestrial telecommunications systems," Publications Office Eur. Union, 1996. [Online]. Available: https://op.europa.eu/en/publication-detail/-/publication/1b803f14-c913-11e6-ad7c-01aa75ed71a1

[21] M. A. Weissberger, "An initial summary of models for predicting theattenuation of radio waves by trees," Electromagn. Compat. Anal., Fort Belvoir, VA, USA, Tech. Rep. ESD-TR-81-101, 1982. [Online]. Available: https://discover.dtic.mil/about/

GLAUCIO L. RAMOS was born in Vitoria, Brazil, in 1974. He received the bachelor's degree in electrical engineering from the Federal University of Minas Gerais, Belo Horizonte, Brazil, in 1999, the master's degree in electrical engineering from the Pontifical Catholic University of Rio de Janeiro, Rio de Janeiro, Brazil, in 2001, the Ph.D. degree in electrical engineering from the Federal University of Minas Gerais, in 2013, and the Postdoctoral degree from the Polytechnic Institute of Leiria, Leiria, Portugal, in 2022. He was a Professor in electronics with the Federal University of Espírito Santo, Sao Mateus, Brazil. Since 2010, he has been with the Federal University of São João del-Rei, Ouro Branco, Brazil, where he is currently an Associate Professor. He has experience in electrical engineering, focusing on electromagnetic theory, radio wave propagation, and antennas. He has authored or co-authored over 70 journal and conference papers in these areas.

NUNO R. LEONOR was born in Leiria, Portugal, in 1988. He received the Licenciatura and Master of Science degrees in electrical and electronics engineering–telecommunications from the School of Technology and Management, Polytechnic Institute of Leiria, Leiria, in 2010 and 2012, respectively, and the Ph.D. degree in teoría de la información y las comunicaciones from the University of Vigo, Vigo, Spain, in 2018. His Ph.D. research program titled "A Generic Doubly-Selective 3D Vegetation Model Using Point Scatterers." He is currently a Researcher with the Instituto de Telecomunicações, Leiria, Portugal; and a Lecturer with the School of Technology and Management, Polytechnic Institute of Leiria, Leiria. His research interests include, but are not limited to, radiowave propagation modeling in the presence of vegetation and wildfires and development of RF measurement systems for characterization of radiowave propagation phenomena, including channel sounders at signal frequencies up to 62 GHz and coverage analysis of fixed and mobile communication systems.

LUIZ DA SILVA MELLO (Member, IEEE) was born in Rio de Janeiro, Brazil. He received the B.S., M.Sc., and Ph.D. degrees in electrical engineering from the Pontifical Catholic University of Rio de Janeiro (PUC-Rio), in 1976, 1977, and 1987, respectively. He was the Dean of the Technology and Sciences School, PUC-Rio, from 2012 to 2020. He is currently the General Manager of PUC-Rio contracts with the industry. He is also an Associate Professor with the Centre of Telecommunication Studies (CETUC/PUC-Rio), since 1977, where he has been involved in teaching and research and development activities on radio propagation measurements and modeling, satellite communications, and mobile cellular systems; and the management of research projects with sponsoring from government agencies, the Brazilian Telecommunications Regulatory Agency, and operators and industries of the telecommunication sector in Brazil. He has published more than 150 research papers in conferences and international journals. He is currently the President of the Brazilian Microwaves and Optoelectronics Society.

FERNANDO J. S. MOREIRA (Senior Member, IEEE) was born in Rio de Janeiro, Brazil, in 1967. He received the B.S. and M.S. degrees in electrical engineering from Catholic University, Rio de Janeiro, Brazil, in 1989 and 1992, respectively, and the Ph.D. degree in electrical engineering from the University of Southern California, Los Angeles, in 1997. Since 1998, he has been with the Department of Electronics Engineering, Federal University of Minas Gerais, Belo Horizonte, Brazil, where he is currently a Full Professor. His research interests include electromagnetics, antennas, and propagation. He has authored or co-authored over 150 journal and conference papers in these areas. He is a member of Eta Kappa Nu and the past President of the Brazilian Microwave and Optoelectronics Society (2014–2016).

CASSIO G. REGO received the degree in electrical engineering from the University of Brasilia, in 1988, the master's and Ph.D. degrees in electrical engineering from the Pontifical Catholic University of Rio de Janeiro, in 1991 and 2001, respectively. He is currently an Associate Professor with the Department of Electronic Engineering, Federal University of Minas Gerais. He has experience in the area of electrical engineering, with an emphasis on electromagnetic theory, microwaves, wave propagation, and antennas, working mainly on the following topics: antennas, radio wave propagation, and applied electromagnetism.

SANDRO T. M. GONCALVES received the Graduate, master's, and Ph.D. degrees in electrical engineering from the Federal University of Minas Gerais, in 2003, 2005, and 2010, respectively, and the Postdoctoral degree from the Ecole Centrale de Lyon, Laboratoire Ampere UMR 5005, in 2016. He was with the Wireless Power Transmission Project. He is currently a Full Professor of undergraduate and graduate education with the Federal Center for Technological Education of Minas Gerais. He has experience in electrical engineering, focusing on telecommunications systems and devices, acting on the following subjects: reflective and wire antennas, finite-difference time-domain method, electronic circuits for ultra-wideband frequency signals, transmission and wireless power reception through rectennas, and auto-resonant dc–dc converters.

RAFAEL F. S. CALDEIRINHA (Senior Member, IEEE) was born in Leiria, Portugal, in 1974. He received the B.Eng. (Hons.) and Ph.D. degrees in electronic and communication engineering from the University of Glamorgan, U.K., in 1997 and 2001, respectively, and the Habilitation degree (Agregacao) from the University of Aveiro, Portugal, in 2020. He has been a Senior Researcher and the Head of the Antennas and Propagation (A&P-Lr) Research Group, Instituto de Telecomunicacoes, Leiria, since 2010; and a Full Professor of telecommunications with the Polytechnic of Leiria, Portugal, since 2001. He has authored or co-authored more than 200 papers in conferences and international journals, two national patents, and four contributions to ITU-R Study Group, which formed the basis of the ITU-R P.833-5 (2005) recommendation. His research interests include studies of radiowave propagation through vegetation media, including wildfires, radio channel sounding, and modeling and frequency selective surfaces for applications at micro- and millimetre-wave frequencies. He was a Senior Member of URSI and a Fellow of IET. He was the Program Chair of WINSYS International Conference, from 2006 to 2012; an Appointed Officer for Awards and Recognitions of the IEEE Portugal Section, in 2014; the Chair of the IEEE Portugal Joint Chapter on Antennas and Propagation-Electron Devices-Microwave Theory and Techniques, from 2016 to 2021; a Regional Delegate of the European Association for Antennas and Propagation (EurAAP) for Andorra, Portugal, and Spain, from 2017 to 2023; and a member of Board of Directors, since 2023. He was an Associate Editor of IEEE TRANSACTIONS ON ANTENNAS AND PROPAGATION, from 2016 to 2022; and *IET on Microwaves, Antennas and Propagation*. He was a member of the editorial board of the *International Journal of Communication Systems* (IJCS) (New York, Wiley).